PAPER

Investigation of fast particle redistribution induced by sawtooth instability in NSTX-U

IOP Publishing | International Atomic Energy Agency Nuclear Fusion

Nucl. Fusion **59** (2019) 086007 (14pp) https://doi.org/10.1088/1741-4326/ab1f20

Investigation of fast particle redistribution induced by sawtooth instability in NSTX-U

D. Kim[1], M. Podestà[1], D. Liu[2], G. Hao[2,a] and F.M. Poli[1]

[1] Princeton Plasma Physics Laboratory, Princeton, NJ 08543, United States of America
[2] Department of Physics and Astronomy, University of California, Irvine, CA 92617, United States of America

E-mail: dkim@pppl.gov

Received 30 January 2019, revised 15 April 2019
Accepted for publication 3 May 2019
Published 21 June 2019

Abstract

The effects of sawtooth on fast ion transport have been studied in reproducible, 2 s long sawtoothing L-mode discharges during the 2016 experimental campaign on National Spherical Torus Experiment Upgrade (NSTX-U) (Menard *et al* 2012 *Nucl. Fusion* **52** 083015). Analysis of the discharges demonstrated that standard sawtooth models (full/partial reconnection models) in the TRANSP code were not capable to fully reproduce the fast ion redistribution induced by sawtooth crashes. Some global parameters such as neutron rate can be recovered while detailed features, e.g. distribution functions, estimated using the models were different from the experimental observation. The standard sawtooth models in TRANSP do not take into account the different effect of sawtooth crashes depending on fast ion energy and orbit type and that may cause the disagreement between experiments and simulations. In this work, the newly developed kick model has been applied to replace the standard sawtooth models for the fast ion transport. TRANSP simulation results using the kick model, taking into account the characteristics of fast ion such as energy and pitch angle, can reproduce experimental neutron rates within 10% difference. The qualitative comparison of the measurements and synthetic diagnostics of fast ion D-alpha (FIDA) and solid state neutral particle analyser (SSNPA) using the TRANSP simulation results with kick model shows good agreements.

Keywords: sawtooth instability, fast ion transport, kick model, TRANSP, NSTX-U

(Some figures may appear in colour only in the online journal)

1. Introduction

The sawtooth instability in tokamak plasmas is a periodic activity characterised by a fast relaxation on time traces of plasma parameters such as temperature and neutron rate and by a following slower recovery of the signal amplitude in the central region where the safety factor q is below unity [1]. The sawtooth instability has an effect on the transport of plasma particles as sawtooth crashes result in the reconnection of magnetic flux surfaces inside the $q = 1$ surface. Thermal particles experience redistribution during the crash along the reconnected flux surfaces. Unlike for thermal particles, the behaviour of fast ions (e.g. α-particles and particles from auxiliary heating systems) is affected not only by the reconnection of magnetic fields but also by the characteristic of fast ions, such as the particle energy and pitch. Therefore, these variables need to be included in sawtooth modelling to understand and to interpret quantitatively the experimental results.

The redistribution of fast ions induced by the sawtooth instability has been investigated in the National Spherical Torus Experiment Upgrade (NSTX-U) [2] experiments. During the 2016 experimental campaign, well-reproducible 2 s long sawtoothing L-mode discharges were obtained [3] providing opportunities to study the fast ion transport during sawtooth crashes in NSTX-U. The experiment results show that the sawtooth-induced redistribution is different based on the fast ion orbit types [4]. The analysis of the experimental measurements from solid state neutral particle analyser (SSNPA) shows that passing particles are strongly affected by sawtooth

[a] Present address: Southwestern Institute of Physics, PO Box 432, Chengdu 610041, China

crashes and redistributions are observed across the plasma minor radius for the whole detectable energy range. On the contrary, the effect of sawtooth crashes on the redistribution is weak for trapped particles. The measured data from fast ion D-alpha (FIDA) spectroscopy confirms the similar behaviour of fast ions. The observations from NSTX-U experiments are qualitatively consistent with those from conventional tokamaks (e.g. DIII-D [5], ASDEX-Upgrade [6–8], TEXTOR [9]) despite the different operation and plasma parameters such as lower magnetic field, smaller machine size, higher β (the ratio of plasma pressure to the magnetic field pressure) and larger $q = 1$ surface. A contradictory result that passing and trapped particles have similar effect from sawtooth crashes is observed in recent MAST experiments [10].

The analysis of NSTX-U sawtoothing discharges has been done using the tokamak transport code TRANSP [11, 12] and the implemented sawtooth models: full reconnection (Kadomtsev) [13] or partial (incomplete) reconnection (Porcelli) model [1]. By choosing a sawtooth model and adjusting free parameters in the model, e.g. fast ion redistribution fraction, partial reconnection fraction, TRANSP simulations can reproduce some global parameters such as neutron rate [4]. However, it is difficult to predict a set of free parameters to match the neutron rate since it cannot be self-consistently evaluated. Furthermore, the agreement of global parameters does not ensure the agreement of estimated features of fast ions such as the fast ion distribution functions. From the tangential fast ion D-alpha (FIDA) measurements [14, 15], it is seen that after a crash fast ions in the centre move outside causing the increase of fast ion population outside the inversion radius. However, the FIDA simulation (FIDASIM) [16] using the TRANSP simulation results that reproduce the experimental neutron rate shows a decrease of the population of fast ions across the whole plasma minor radius [4].

The discrepancy of fast ion distributions between the measurements and the simulation may result from that the sawtooth models in TRANSP do not take into account the characteristics of fast ions. Simulation works using the ORBIT code [17], which takes into account the fast ion properties such as fast particle energy and orbit type, confirm the experimental observation that passing particles in the core region are expelled and move outside the $q = 1$ surface while a sawtooth crash does not have significant effects on trapped particles, in particular for the particles with energy higher than 30 keV [18]. Therefore, a more reliable model that includes the effect of fast ions energy, orbit type and other phase space variables is required to evaluate the behaviour of fast ions during sawtooth crashes more quantitatively in the TRANSP simulations.

In this work, we have extended the previous work [18] by implementing the newly developed kick model [19, 20] into the ORBIT code. The kick model computes the probability matrix of change of fast ion energy and angular momentum in the presence of sawtooth instability in the ORBIT calculation. By using the probability matrix as an updated input parameter for NUBEAM module [21, 22] in TRANSP, the effect of phase space variables on the modelling of sawtooth-induced fast ion transport can be included in time dependent simulations. TRANSP simulation results using the kick model show features of sawtooth-induced fast ion redistribution that are not found from the conventional sawtooth models. In addition, from the FIDASIM results, the comparison with experimental observations are carried out. The preliminary test results confirm that energy, canonical angular momentum, pitch should be included in the modelling to describe the behaviour of fast ions in sawtoothing discharges.

The rest of this paper is organised as follows. The experimental scenario of the NSTX-U discharge is summarised in section 2 with the main diagnostics for fast ions and the simulation tools applied in this work. The applied perturbation model and an example of kick model application will be discussed in section 3. The sensitivity of the choice of mode amplitude is also investigated. In section 4, the comparison of TRANSP simulation results using different models are shown and the comparison with experimental measurements and theoretical prediction will be discussed in section 5. Finally, the conclusion follows in section 6.

2. Experimental scenario and simulation tools

Simulations have been performed based on the NSTX-U L-mode sawtoothing discharge #204163, a center-stack limited L mode plasma with a flat-top plasma current I_p of 700 kA and a toroidal magnetic field B_T of 0.65 T at the magnetic axis ($R_0 \sim 1.05$ m). The experimental scenario is displayed in figure 1. The time trace of plasma current I_p shows the ramp up (up to about 300 ms) and flat-top phases. The injected neutral beam power P_{NB} of 1.1 MW with the injected energy of 72 keV is applied from a perpendicular beam source (1B) with tangency radius of 60 cm from the ramp-up phase to the end of discharge. The sawtooth activities with period of 30–40 ms are seen from the repetitive drop of neutron rate and the spikes on magnetic fluctuations from Mirnov coils. Electron temperature T_e (blue) and density n_e (red) profiles averaged over 10 ms before (solid) and after (dashed) a crash at 1353 ms are shown in figure 1(*e*). Due to the crash, T_e and n_e profiles drop inside the $q = 1$ surface near the major radius R of 130–135 cm (normalised minor radius ~0.4) while slightly increase outside the inversion radius.

As the sampling times of diagnostics are comparable to the sawtooth periods (16 ms for Thomson scattering system [23] and 10 ms for charge exchange recombination spectroscopy (CHERS) [24]), available profile data cannot fully reflect the effect of sawtooth crash. Therefore, the measured profile data are re-processed through conditional average to reconstruct the evolution of profiles during sawtooth cycles on a finer time grid. Profiles are first re-scaled based on a 100 ms running average at each radial point to remove their long-time-range evolution. Then the conditional average is performed on the *profile variation* to infer the characteristic time-scale for profile recovery. Finally, experimental data are used to constrain the reconstructed profile at each sawtooth crash based on the inferred recovery time-scale. Once the typical recovery time is determined, the profile reconstruction is based on a two parameter fit of the available data, where the fitting parameters are the amplitude of the density/temperature drop and

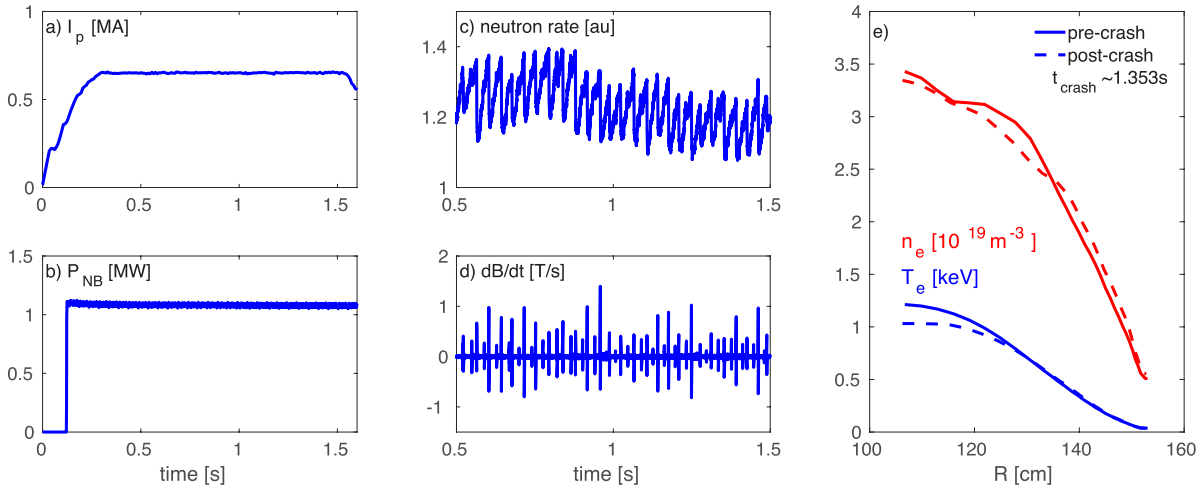

Figure 1. Experimental scenario for NSTX-U discharge #204163. (*a*) Plasma current in ramp-up and flat-top phase. (*b*) Time trace of injected NB power of 1.1 MW from beam source 1B. (*c*) Measured neutron rate in flat-top phase where sawteeth were detected. (*d*) Magnetic fluctuations from Mirnov coils. (*e*) Example of electron density (red) and temperature (blue) profiles reconstructed through conditional average before (solid) and after (dashed) a sawtooth crash at $t = 1353$ ms.

the average value (offset) of density/temperature for each specific sawtooth event. For events for which not enough profile data are available, the amplitude of the drop is instead constrained from SXR data, rescaled to match the drop for events with sufficient density/temperature time points.

The fast ion diagnostics used in this work include neutron detectors, solid state neutral particle analyser (SSNPA) arrays [25, 26] and fast ion D-alpha (FIDA) spectroscopy [14, 15]. The neutron detector has been used for the measurements of the volume-integrated neutron flux. On NSTX-U about 90% of neutrons are produced by beam-target (thermal) reactions, thus the drops in neutron rate can indicate changes of thermal and/or fast ion profiles during sawtooth crashes. The SSNPA diagnostic measures neutral particle fluxes generated from charge exchange (CX) reactions between fast ions and neutrals. The FIDA diagnostic measures the Doppler shifted D-alpha emission of re-neutralised fast ions from CX reactions with beam injected neutrals or background cold neutrals. The FIDA system consists of toroidally viewing t-FIDA and vertically viewing v-FIDA for mostly detecting signals from passing and trapped particles, respectively. The SSNPA and FIDA diagnostics can have active and/or passive signals that use CX reactions with injected beam neutrals and background neutrals. The active signals originate near the intersection of the diagnostic sightlines and the injected neutral beam footprint. The passive signals mainly come from the plasma edge since the background neutral density is usually a few order higher in the edge region than in the core.

In order to test the dependencies of fast ion redistribution during sawtooth crashes on the fast ion phase space variables, the ORBIT code [17] has been used in conjunction with the reduced kick model [19, 20]. ORBIT is a Hamiltonian guiding-centre code for analysing energetic particle transport induced by instabilities in tokamak plasmas. In this work, we have applied $m = 1$, $n = 1$ mode magnetic field perturbations to represent sawtooth instability. The kick model evaluates transport probability matrices to represent the fast ion transport by instabilities. Using the estimation from the ORBIT code in the presence of sawtooth instability, the kick model computes the probability matrices that represent the change of particle's energy (ΔE) and canonical angular momentum (ΔP_ζ) around a certain position in phase space (E, P_ζ, μ_0, the magnetic moment) during their orbiting over a certain time interval. Note that the change of μ_0 is not computed as it is assumed to be constant.

The resulting probability matrix $p\left(\Delta E, \Delta P_\zeta | E, P_\zeta, \mu_0\right)$ from the kick model can be used as input for time dependent transport simulations, such as TRANSP [11, 12] used for this work. TRANSP is a transport code that enables time dependent integrated interpretative/predictive simulations of tokamak discharges. The implemented Monte Carlo module NUBEAM [21, 22] computes the dynamics of energetic particles. The kick model results are used as an updated input value to the NUBEAM module to include the effects of sawtooth instability. NUBEAM uses $p\left(\Delta E, \Delta P_\zeta | E, P_\zeta, \mu_0\right)$ and the given mode amplitude to update the evolution of fast ion E, P_ζ, which affects the fast ion distribution functions, density, etc.

To compare fast-ion distribution functions predicted using kick model and the standard sawtooth models, synthetic fast ion diagnostic signals are calculated by the FIDASIM code [16] and compared with the experimental FIDA and SSNPA signals. The FIDASIM code models neutral beam deposition and can predict active and passive FIDA and SSNPA diagnostic signals, treating all relevant atomic physics such as charge-exchange, atomic excitation and ionisation processes. The main inputs are plasma equilibrium, neutral beam parameters (geometry, power waveform), fast ion distribution and plasma profiles.

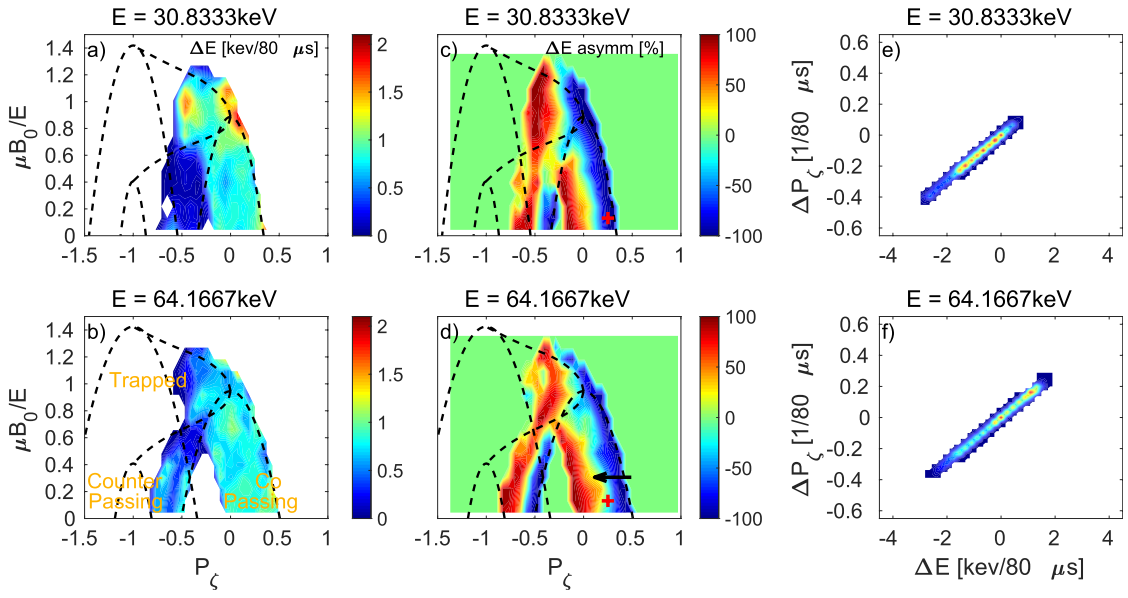

Figure 2. (*a*) and (*b*) The averaged root-mean-square of the particle energy change due to a sawtooth crash. (*c*) and (*d*) The balance of the averaged positive and negative energy kicks at each location. The black dashed lines are the boundary of different orbit types. (*e*) and (*f*) Calculated probability matrices from the kick model for two energy cases at a certain location on the fast ion phase space (Red crosses in (*c*) and (*d*)).

3. ORBIT modelling with kick model

The ORBIT code has been used to investigate the characteristics of fast ion redistributions and to compute the transport probability matrix in the presence of sawtooth instability. The sawtooth instability is represented by a linearised radial displacement ξ (see [18]). In the ORBIT code the magnetic perturbation is described using a scalar function α and only the radial component of perturbed field is considered in this work. Thus the radial profile of ξ has been converted into α using the relation between them [27] (See equations (1*a*) and (1*b*)) and the radial component of applied perturbed magnetic field is shown in equation (1*c*)

$$\delta\vec{B} = \nabla \times \left(\alpha\vec{B}\right), \tag{1a}$$

$$\alpha_{mn}\left(\psi_p\right) = \frac{m/q - n}{mg + nI}\xi_{mn}\left(\psi_p\right), \tag{1b}$$

$$\delta\vec{B}\cdot\nabla\psi_p = \sum_{m,n}\frac{mg + nI}{J}\alpha_{mn}\left(\psi_p\right)\cos\left(n\zeta - m\theta - \omega t\right), \tag{1c}$$

where $\vec{B}$ and $\delta\vec{B}$ are the equilibrium and the perturbed magnetic field, respectively, (m, n), (θ, ζ) and (g, I) are the poloidal and toroidal mode numbers, angles and current functions, respectively, q is the safety factor, ψ_p is the poloidal flux, J is the Jacobian and ω is the mode frequency. In this work, a constant ω value of 10 kHz, the average frequency in lab frame during sawtooth cycles, is applied.

Using the given magnetic perturbation, the kick probability matrix has been calculated in the ORBIT code for each sawtooth crash. Note that for the kick model application, the mode amplitude is fixed in time so that only just before and after a crash cases are considered. The time dependent mode amplitude in TRANSP will be discussed in section 4. One example of the kick model application from a time slice (1353 ms) is shown in figure 2. In figures 2(*a*)–(*d*), the canonical angular momentum (P_ζ) and the ratio of the magnetic moment to the particle energy ($\mu B_0/E$) are used for the horizontal and the vertical axes, respectively. The black dashed lines indicate the boundary of orbit type classification defined using the Hamiltonian equation of motion and the conservation of P_ζ [28]

$$\begin{aligned} E &= \rho_\parallel^2 B^2/2 + \mu B + \Phi, \\ P_\zeta &= g\rho_\parallel - \psi_p, \end{aligned} \tag{2}$$

where $\rho_\parallel = v_\parallel/B$ the normalised parallel gyro radius, Φ the electrostatic potential. Note that the right curve indicates the boundary near the magnetic axis and the black arrow in figure 2(*d*) indicates the real space direction from the magnetic axis to the edge.

Figures 2(*a*) and (*b*) represent the averaged root-mean-square of the particle energy change due to a sawtooth crash in terms of phase space variables. For two different energy ranges (~30 and ~65 keV), passing particles are clearly affected by a crash while for trapped particles a sawtooth crash has less effect on higher energy case. As the critical energy for the redistribution [29] of trapped particle is about 30 keV (discussed in section 5) for this plasma, the change in phase space is limited for higher energy. On the other hand, since the critical energy of passing particles is much higher than the neutral beam injection energy (~70 keV), most of passing particles are redistributed by sawtooth instability.

From figures 2(*c*) and (*d*) one can infer the redistribution of fast ions with different orbit type and energy. These figures show the balance of the averaged positive and negative

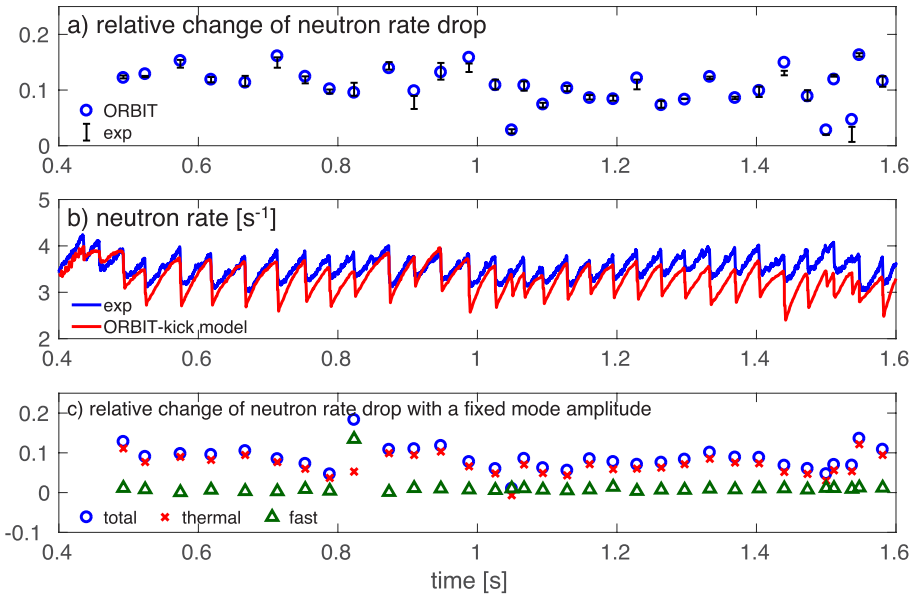

Figure 3. (*a*) Mode amplitude can be determined by the comparison of the simulated relative change of neutron rate before and after a crash with the measurement. (*b*) The neutron rate from TRANSP simulation (red) using a kick probability matrix with normalised mode amplitudes is over-estimated compared to the measured neutron rate (blue). (*c*) Deuterium density accounts for most of the relative change of neutron rate. Thus the uncertainties in deuterium density estimation should be reduced to have more accurate mode amplitude calculation.

energy kicks at each location. Note that from the relation between ΔE and ΔP_ζ ($\Delta P_\zeta/\Delta E \sim n/\omega$), the positive (negative) energy kicks correspond to positive (negative) P_ζ kicks. In addition, from equation (2), one can infer $\Delta P_\zeta \propto -\Delta\psi_p$. The phase space location where ΔE is mostly negative is displayed with blue colour while red indicates mostly positive change of energy on average. Using the relation between ΔE, ΔP_ζ and $\Delta\psi_p$, one can picture in the real space that particles are expelled from near axis (blue region near the axis boundary, positive $\Delta\psi_p$) or move inside (red outside the $q = 1$ surface, negative $\Delta\psi_p$) during a crash based on their initial position with reference to the inversion radius (green region between the blue and red). The detail of kick probability for the redistribution of fast ions are shown in figures 2(*e*) and (*f*) (red crosses from the blue and green regions in figures 2(*c*) and (*d*)). The probability is calculated for a time step of 80 μ s in the ORBIT modelling. As the chosen phase space location is in blue region in figure 2(*c*), the variations of P_ζ and E for lower energy passing particles near the magnetic axis in real space are mostly negative; this indicates that particles are expelled from the centre due to a crash. For the higher energy case, the averaged positive and negative probabilities are balanced. In this case as the same P_ζ and E position is shifted in phase and real space, particles are located near the inversion radius so that passing particles have similar probability to move inside and outside the $q = 1$ surface. Unlike passing particles, the probability matrices for trapped particles are expected to be mostly positive (larger red area in figure 2(*c*)) although the change in (P_ζ, E) is lower for higher energy particles.

In the perturbation model, the nominal mode amplitude is a free parameter. The mode amplitudes of each crash can be determined by comparing the relative change of neutron rate drops with measurements. The relative change of neutron rate drops from ORBIT results is evaluated using the calculation of D–D reaction rate [18]

$$\Delta\text{neut\_rate} = \frac{\sum_k^{N_0} n_{d0,k} S_{0,k} \sqrt{E_{0,k}} \mathrm{d}V_k - \sum_k^{N_f} n_{\mathrm{d}f,k} S_{f,k} \sqrt{E_{f,k}} \mathrm{d}V_k}{\sum_k^{N_0} n_{d0,k} S_{0,k} \sqrt{E_{0,k}} \mathrm{d}V_k}. \tag{3}$$

The deuterium density n_d is evaluated from the conditionally averaged n_e and the plasma volume element $\mathrm{d}V$, the reaction cross section S and the particle energy E are computed in ORBIT code. Using the ORBIT-estimated mode amplitudes, the relative change of neutron rate drops can reproduce the measured ones as shown in figure 3(*a*).

To verify the feasibility of the estimated mode amplitude, kick probability matrices are evaluated for each sawtooth crash using the mode amplitudes and are applied to TRANSP simulation. Due to the limited number of input parameter in TRANSP, only one matrix at a certain time slice is used for all sawtooth crashes. The different mode amplitudes for all crashes are normalised by the mode amplitude of chosen time slice. In TRANSP, the probability matrix and the normalised mode amplitudes are used as input data. More details of TRANSP simulation will be discussed in section 4. The evaluated neutron rate (red) is shown in figure 3(*b*) with the experimental data (blue). Unlikely to the relative change of neutron rate drop using the estimated mode amplitudes, the resultant neutron rate does not reproduce the experimental measurements but is over-estimated (the change of neutron rate at each sawtooth crash is larger than the measured one). A possible explanation would be the uncertainties for the estimation of mode amplitudes. As the calculation of the

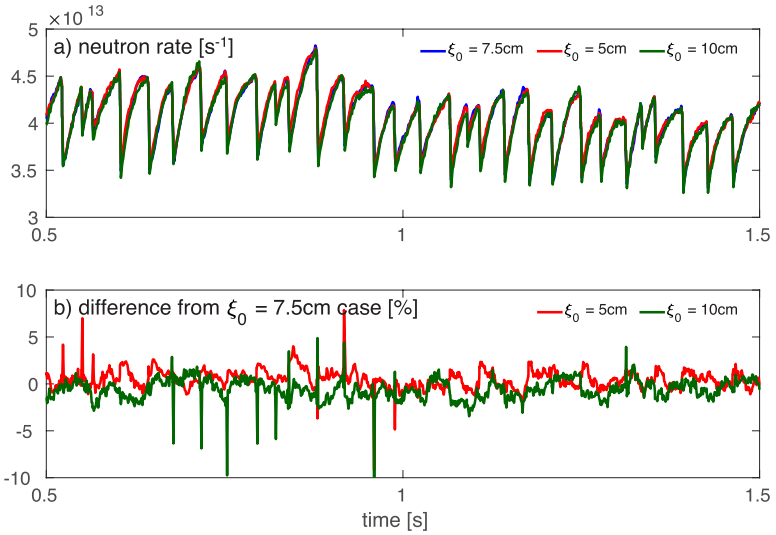

Figure 4. (*a*) Neutron rate from TRANSP simulation using kick probability matrix with $\xi_0 = 7.5$ cm (blue), 5 cm (red) and 10 cm (green). All three cases are almost the same. (*b*) The differences in simulated neutron rate between $\xi_0 = 7.5$ cm and 5 cm (red) and $\xi_0 = 7.5$ cm and 10 cm (green) are less than 5%. The mode amplitude in kick model may have little effect on the TRANSP simulations.

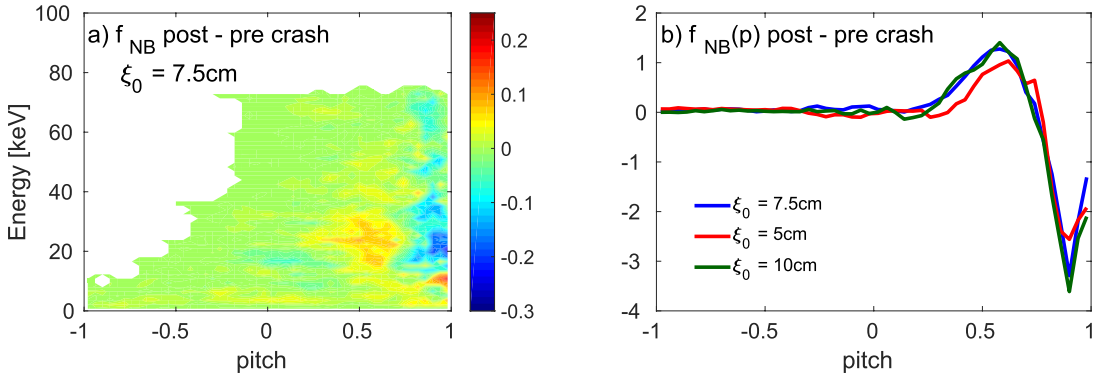

Figure 5. (*a*) The difference of fast ion distribution before and after a sawtooth crash evaluated outside the inversion radius for $\xi_0 = 7.5$ cm case. (*b*) The difference of distribution functions for three ξ_0 cases are integrated over the all energy range. The 1D distribution functions (function of pitch) are within 10%–15% difference so that in this work, the mode amplitude is fixed to 7.5 cm.

relative change of neutron rate drops is based on the reaction rate between thermal and fast particles, most of contribution of the estimated value comes from the thermal plasma density (figure 3(*c*)). As previously mentioned, the profile data are re-processed through conditional average. Due to the process, thermal particle profile can have uncertainties that may cause an incorrect estimation of the relative change of neutron rate drops. For more accurate simulations, the time resolution of plasma density and temperature measurements should be increased to reduce the uncertainties.

Therefore, in the rest of this work, a fixed nominal mode amplitude has been used for the probability matrix calculation. The default value of the nominal mode amplitude ξ_0 of 7.5 cm has been taken from the previous work [18]. Since this value has also been estimated based on the same analysis with uncertainties (comparison of the relative change of neutron rate drop), it is worth to have sensitivity tests of given mode amplitude using $\xi_0 = (7.5, 5, 10\,\text{cm})$. The probability matrices with the three ξ_0 values are computed and are applied to TRANSP simulations. First, the neutron rate has been compared (figure 4(*a*)). Despite about 30% change of the nominal mode amplitude in kick model calculation, the resultant neutron rates are almost the same. The differences of neutron rate between $\xi_0 = 7.5$ cm and other cases (figure 4(*b*)) are less than 5% and therefore show the weak dependence on mode amplitude.

Since the neutron rate is not sufficient to investigate the effect of mode amplitude, another test using fast ion distributions has been carried out. The difference of fast ion distribution functions before and after a crash at the normalised radius of 0.55 (outside the inversion radius) for $\xi_0 = 7.5$ cm case is shown in figure 5(*a*). The number of fast ions along the entire energy range are integrated at each pitch values to compare three cases. As shown in figure 5(*b*), the change of fast ion distribution before and after a crash are almost the same. For $\xi_0 = 5$ cm case, the difference is about 10%–15% and as the mode amplitude increases the difference becomes smaller (saturation of the effect of increasing mode amplitude).

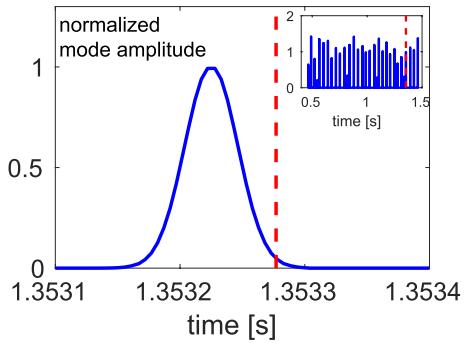

Figure 6. Normalised mode amplitude at 1353 ms shows the input data of mode amplitudes for all sawtooth crash times (inset) in TRANSP.

Therefore, one can conclude that for this scenario the results from the kick model are not very sensitive to the assumed mode amplitude. For the rest of simulations in this work, the fixed nominal mode amplitude of $\xi_0 = 7.5$ cm has been used for the kick model application in ORBIT.

4. Application of kick model to time dependent transport simulations

The calculated kick probability matrix has been applied to time dependent TRANSP simulations to test the improvement of the modelling for the fast ion redistribution induced by sawteeth. The sawtooth crash time is identified from the measurements of the soft x-ray and is given as an input parameter for the simulations. The modification of thermal plasma temperature and density profiles during sawtooth cycles is included in the conditional averaged input profiles. For the target discharge, the motional Stark effect (MSE) measurements were not available thus the q profile and its temporal evolution are evaluated by solving the poloidal field diffusion equation using a fixed boundary equilibrium code TEQ [30]. Note that kick model is applied only for fast ion transport so that the modification of q profile is described by the conventional sawtooth models (full [13] and partial [1] reconnection models).

The prediction of fast ion redistribution is described based on the chosen model. Using the result from ORBIT/kick modelling, NUBEAM module has an additional input of $\Delta P_\zeta, \Delta E$ to take into account the phase space variables for the sawtooth-induced redistribution. Although the probability matrices are computed for each sawtooth crash, due to the limit of number of input data in TRANSP and for simplicity, only one matrix (from 1353 ms) is used for all the crash times. As previously discussed, ORBIT-estimated mode amplitudes brought over-estimated neutron rate drops due to uncertainties. Thus the fixed nominal mode amplitude of $\xi_0 = 7.5$ cm is applied for the probability matrix calculation in ORBIT/kick modelling and the normalised mode amplitudes for each crash time in TRANSP are determined using the relative change of measured neutron rate drops (normalised by the amplitude at 1353 ms). The normalised mode amplitude at 1353 ms is shown in figure 6 with the sawtooth crash time (red dashed line) and other normalised amplitudes in the inset. It is assumed that the perturbation is applied just before the crash since the probability matrix is computed based on the equilibrium before the crash time. This assumption may not correctly reflect the physics of sawtooth instability that the effect of sawtooth on the fast ion redistribution mostly occurs during the 'fast phase' after a crash. As discussed in [18], the time dependent mode amplitude can be applied to kick model in the ORBIT code and the effect of sawtooth can be included more accurately. However, in this work, the main idea of using a reduced kick model is to simplify the calculation considering reduced number of parameters. More detailed approach which covers the physics may be needed for the further study. Fast ion redistributions can also be described in TRANSP using conventional sawtooth models with chosen free parameters. The simulation results using different models are compared in the following.

In figure 7, the time traces of neutron rate from TRANSP simulations using different models are shown. On the upper panel, blue, red and green lines indicate the measured neutron rate, TRANSP simulation results without fast ion redistribution and with kick model, respectively. On the bottom one, blue curve is the same and purple and light blue ones are full and partial reconnection cases. In this work, the fraction of fast ion redistribution is set to 20% and 50% for the full and partial reconnection cases, respectively. A partial reconnection fraction of 50% is used. Note that the free parameters are determined to match the measured neutron rate. The measured neutron rate is normalised to have the same averaged value as TRANSP simulations between 360 and 440 ms, where no MHD activity has been detected.

The neutron rate from the TRANSP simulation in which the effect of sawteeth on fast ions is suppressed (red) is comparable with the measured one (blue). This indicates that the change in the thermal plasma profile has the most contribution to the neutron rate drop. The application of kick model (green) brings slightly better agreement but the effect of fast ion redistribution on the neutron rate drop is not significant. Using the conventional sawtooth models, the neutron rate similar to the reference case can be produced with a proper set of free parameters; the fraction of fast ion redistribution, the partial reconnection fraction. Since these free parameters cannot be self-consistently determined, predictive modelling for sawtooth-induced fast ion redistribution is demanding using the conventional models.

From figure 7, it seems that the conventional models can be used to describe the fast ion redistribution in sawtoothing plasmas. However, although the simulated neutron rates using the different models are comparable to the measured one, detailed features are not similar. Several profiles related to the fast ion evolution 2 ms before (solid) and after (dashed) a crash at 1353 ms from kick model (blue), full (red) and partial (green) reconnection cases are compared in figure 8. Since the kick model does not affect the q profile, full reconnection model is applied as a default setting. As the central value of the q profile from partial reconnection stays below unity after a crash, the profile before crash is more relaxed compared to the profile from full reconnection. The estimated fast

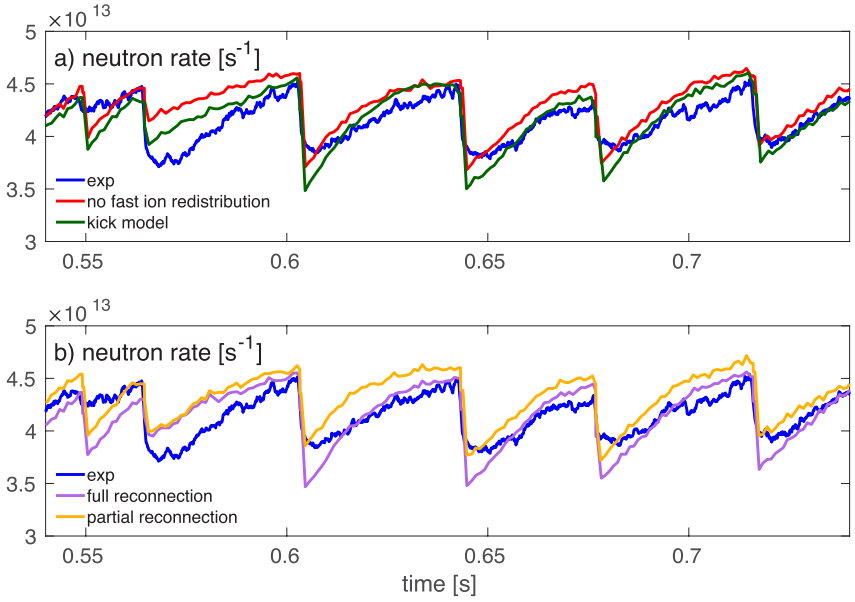

Figure 7. (*a*) Neutron rates from the measurements (blue), without fast ion redistribution (red) and kick model (green). It is confirmed that the main contribution to the change of neutron rate comes from the variation of thermal plasma. Using the kick model, the neutron rate shows better match but both cases are in a good agreement with the measurements within errorbar. (*b*) Neutron rates from the measurements (blue), full (purple) and partial (yellow) reconnection cases. By adjusting free parameters, the conventional sawtooth models can provide neutron rates close to the experimental value.

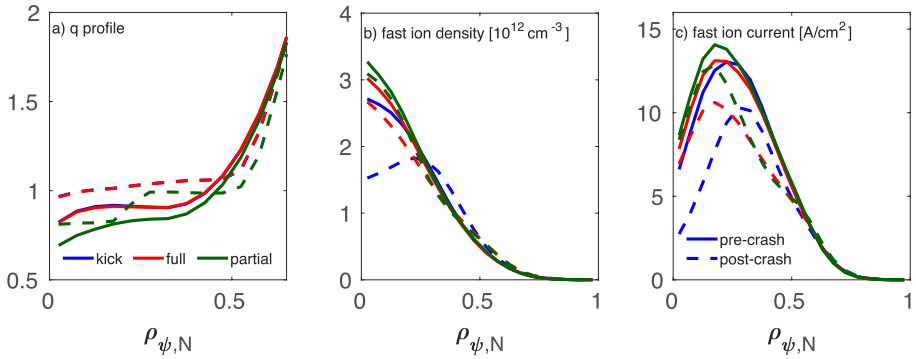

Figure 8. (*a*) Safety factor q (*b*) fast ion density (*c*) fast ion driven current profiles from each model (blue—kick model, red—full reconnection, green—partial reconnection) before (solid) and after (dashed) a crash. Using kick model, clear effect from a sawtooth crash is seen on the profiles. Since kick model does not affect q profile, full reconnection is assumed.

ion density profiles in figure 8(*b*) clearly show the difference among the models. The post-crash profile from the kick model demonstrates the effect of sawtooth on the redistribution. The central density drops while density outside inversion radius increases. Note that the inversion radius is inside the $q = 1$ surface location. Full and partial reconnection cases have similar fast ion density profiles. After a crash, density profile at the centre is slightly diminished but the difference is small as the redistribution fraction is small. Since more than half of fast ions are not modified by the sawtooth crash (redistribution fraction <50%), the post-crash profile keeps almost the same shape. Similar difference can be seen in the NB driven current density profile (figure 8(*c*)).

The fast ion distribution functions just outside the $q = 1$ surface ($\rho_{\psi,N} = 0.55$) before and after a sawtooth crash shown in figure 9 also illustrate the difference between applied models. Figures 9(*a*) and (*b*) are the fast ion distributions from the kick model before and after a crash while figures 9(*c*) and (*d*) are the partial reconnection case. Note that full and partial reconnection cases have similar distribution functions thus only partial reconnection case is shown here. The kick model results confirm that the sawtooth crash redistributes fast ions in both radius (as shown in figure 8(*b*)) and energy, in particular the low energy passing and trapped particles. Passing particles with larger pitch decrease about 20%–30% while trapped/passing particles with pitch around 0.5 increase about 50%. This may indicate that passing particles change their orbit type and become trapped particles as discussed in [18]. However, as seen in figure 2, particles move around the inversion radius and that can result in the change of the local distribution of fast ions. Therefore, for the precise analysis, the tracking of particles and the change of orbit type are required.

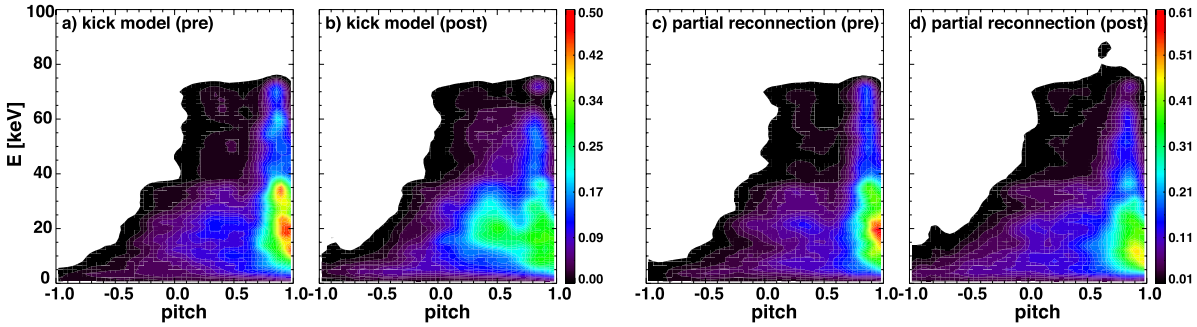

Figure 9. The distribution of fast ion at $\rho_{\psi,N} = 0.55$ (*a*) and (*b*) from kick model before and after a crash and ((*c*) and (*d*)) from partial reconnection (50% reconnection fraction, 50% fast ion redistribution). From kick model, the population of passing particles with high pitch decreases while that of trapped particles increases. For the partial reconnection case, passing particles have the same behaviour but no clear change of trapped particles is found.

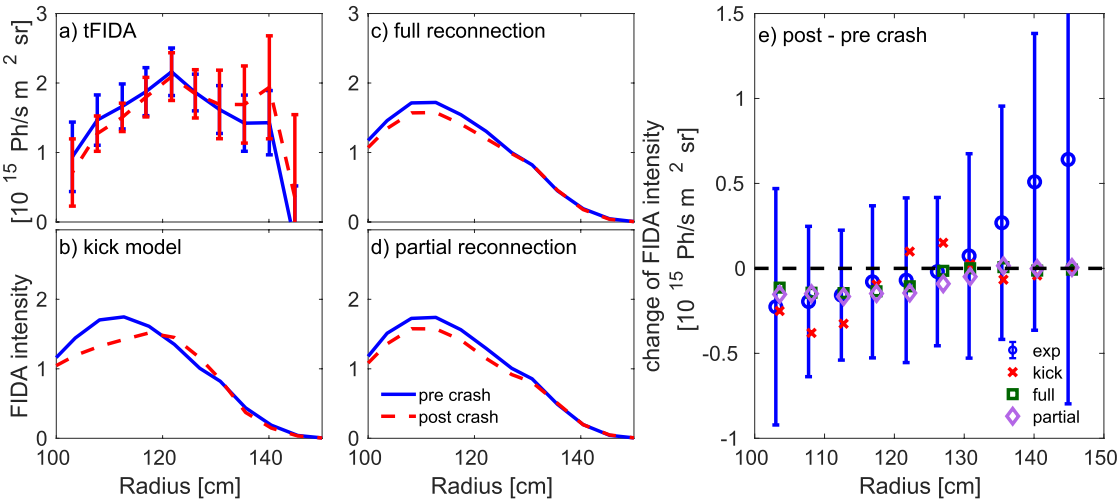

Figure 10. The comparison of simulated t-FIDA spatial profiles with (*a*) experimental FIDA data before and after a sawtooth crash using (*b*) kick model (*c*) full reconnection and (*d*) partial reconnection. All profiles are averaged over three time steps (1, 3, 5 ms) before and after a crash. (*e*) The change of profiles after a crash is shown for the experimental and simulation results. Using kick model, qualitative features of the fast ion distribution modification due to a sawtooth crash are reproduced.

In addition to the increase of the lower energy (<40 keV) in the lower pitch range (0–0.5), the number of higher energy particles is extended as well as the increase of counter passing particles (pitch $\leqslant -0.5$). On the other hand, the distributions from partial reconnection do not have a significant variation. The number of the low energy passing particles with pitch ~1 decreases but no clear change in trapped particles. Similar to the kick model case, particles with middle pitch range become more but compared to the kick model case, the increment is much smaller. In addition, as previously discussed, trapped particles (pitch ~ 0) with higher energy over ~40 keV are not affected by sawtooth as the distribution function does not change much for both case.

5. Comparison with the experimental measurements and theory

5.1. Comparison with measurements: FIDA and SSNPA

As discussed in section 4, the kick model takes into account the phase space dependence of fast-ion transport during sawtooth crashes. It can result in some different features in fast-ion distribution that are not observed with the conventional sawtooth models, as shown in figures 8 and 9. In order to validate the improvement from the kick model, the simulation results are compared with the experimental measurements [4]. The fast-ion distribution functions calculated by TRANSP with different sawtooth models are used as inputs to the synthetic diagnostic code FIDASIM [16]. Figure 10(*a*)–(*d*) shows the measurements and simulations of the tangentially-viewing FIDA (t-FIDA) diagnostic, which is mainly sensitive to passing particles, before and after sawtooth crashes. For the experimental data, only the data from tangentially-viewing FIDA system is shown although the FIDA diagnostic on NSTX-U has both tangentially- and vertically-viewing FIDA systems (t-/v-FIDA). In these sawtooth discharges, the v-FIDA data is available only for the outer channels ($R_{\mathrm{maj}} \geqslant 110$ cm) and the change of v-FIDA signal during sawteeth is within the experimental uncertainties. The experimental data and the errors bars in figure 10(*a*) are averaged over seven sawtooth cycles to get better statistics. In the three simulations, kick model, full and partial reconnection sawtooth models are applied

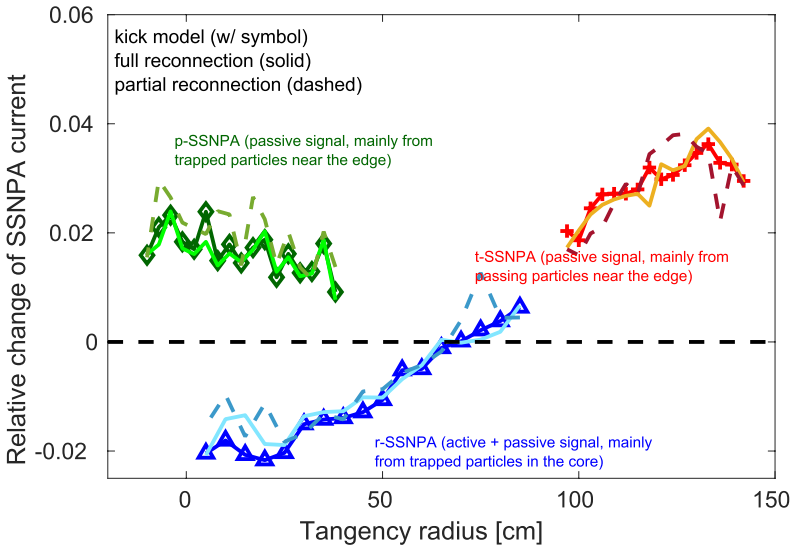

Figure 11. The relative change of synthetic SSNPA diagnostic signal after a crash from p-SSNPA (greenish colours), r-SSNPA (bluish colours) and t-SSNPA (reddish colours) using kick model (symbols), full (solid) and partial (dashed) reconnection models. Since there is no active neutral beam intersecting with the sightlines of p-SSNPA and t-SSNPA systems in this case, all the signals are from the passive contributions near the plasma edge. The r-SSNPA systems views the injected NB source, thus the signal is the combination of active contribution from the plasma core and passive contribution from the plasma edge.

respectively for comparison. The simulations calculate the FIDA spatial profile 1, 3, 5 ms before (blue solid) and after (red dashed) the sawtooth crash at 1353 ms and then average over these three time slices since the temporal resolution of FIDA diagnostics is 10 ms. Note that the error bars of simulations are not displayed since the variations between those time slices are negligibly small.

Despite the relatively large level of error bars, one can clearly see the effect of sawtooth instability on the fast ion distribution function from the t-FIDA measurement: some fast ions are redistributed from the central region to the region outside inversion radius after the crash. Since all the three simulations have similar neutron rate drops and use the same thermal plasma profiles as input, one may expect that the fast-ion distributions would also be similar. However, this is not the case. Figure 10(*b*) shows that the t-FIDA signal from the simulation with kick model decreases in the central region and increases at the region outside the inversion radius after the sawtooth crash. The simulated t-FIDA signals from the other two conventional sawtooth models shows a weak depletion across the whole minor radius without any sign of increase in the edge. It should be mentioned that the relative measurements are more accurate than absolute FIDA measurements. The measured FIDA profile is generally broader than the simulated FIDA profile even in the absence of sawteeth, which is also observed on NSTX [31]. Thus it is worthy to compare the experimental change of FIDA signals due to sawtooth crashes with simulations. Although the error bars of the experimental change are large, one can qualitatively compare the averaged values. As shown in figure 10(*e*), the kick model exhibits a similar trend as the experimental change till the region near the sawtooth mixing radius, but nearly zero in the edge region. Although the kick model shows an increase of FIDA signal near 120–130 cm, it does not see the large increase in the edge region as observed in the experimental data. This discrepancy can be resulted from the shape of magnetic field perturbation (no perturbation outside the $q = 1$ surface) as well as from the large fraction of redistribution of the centrally located passing particles. The changes of FIDA signals predicted by the other two conventional sawtooth models stay below zero within the mixing radius and have the similar trend as the kick model case near the edge region. The simulations suggest that taking the phase space variable into account can improve sawtooth modelling to describe fast ion transport more reliably. In addition, it also shows that the match of neutron rate is not a sufficient prerequisite to test sawtooth models since fast ion transport in phase space and resulted fast ion distribution could be be different. Note that the redistribution fractions of fast ion for full and partial reconnection are set to 20% and 50%, respectively. With higher fractions, the change of FIDA signal may be similar to kick model but the neutron rate would show a larger discrepancies with respect to the measurements, with a large over-estimate of the neutron rate drops.

The FIDASIM simulations for the synthetic SSNPA diagnostic are also performed to compare with the experimental SSNPA measurement. From the experiments, a significant increase of t-SSNPA signals (mainly passive signal from CX reactions near the plasma edge between passing fast ions and background neutrals), a small increase of p-SSNPA signals (mainly passive signal from trapped fast ions near the plasma edge) and a very weak reduction of r-SSNPA signals (dominated by active signal from reactions between trapped fast ions and neutrals from neutral beam injection in the plasma core) have been observed after each sawtooth crash. Since the relative change of t-SSNPA signal is a few times larger than that of r-SSNPA or p-SSNPA, it was concluded that passing particles are affected by sawtooth [4].

Figure 11 shows the SSNPA signals predicted from three simulations using kick model (symbols), full (solid) and partial (dashed) reconnection models. Although the kick models and full reconnection model produce slightly more similar trends for all three SSNPA subsystems, the difference between three sawtooth models are relative small and comparable with the channel-to-channel variation. All the SSNPA simulations predict a weak reduction of r-SSNPA and a small increase of p-SSNPA signals, i.e. some trapped particles are redistributed from the plasma core to the outer region. The passive t-SSNPA signals are predicted to increase in a similar level for all three sawtooth models, which indicates a increase of the population of passing fast ions near the edge. Note that although the change of t-SSNPA signal is larger than p-SSNPA or r-SSNPA, the enhancement of t-SSNPA signal is still weaker compare with measurements. The magnitude of change of the SSNPA signals is a few times smaller than the measurements for all three sawtooth models although the overall trend is qualitatively consistent with the experimental observations.

One likely reason why the SSNPA simulations cannot differentiate the three sawtooth models is that the passive SSNPA signals (p- and t-SSNPA) are mainly from the plasma edge due to the high background neutral density. Because there is no magnetic perturbation outside the $q = 1$ surface for all three sawtooth models and that the most affected region of fast ion distribution due to sawtooth is within and near the $q = 1$ surface, the passive signals cannot reflect the difference between models. Note that for the FIDA diagnostic, the comparison is for active signals from the intersection area of neutral beam and FIDA sightlines and the passive signals were subtracted out through beam modulation method.

Another possible reason is the huge uncertainty of background neutral density profile and absolute magnitude. In the passive SSNPA simulations, background neutral density is typically extracted from TRANSP results in which the neutral density is calculated with a simple 1D model FRANTIC. For this case, the TRANSP calculated neutral density decreases after a sawtooth crash an then recovers. This is quite different from experimental observations. In experiments, the edge D-alpha emission is observed to burst at a sawtooth crash (likely due to increase of source of neutrals when particles hitting the wall) and gradually return to pre-sawtooth level. In order to reduce the uncertainty, the same background neutral density profile is used for the time slices before and after a sawtooth crash in all the SSNPA simulations. For better understanding, diagnostics need improvement to see the reaction in the core region and it can also be helpful to improve the neutral density calculation module in TRANSP.

5.2. Comparison of critical energy for the redistribution of fast particles

The simulation results of the kick model application can be compared with the theoretically estimated critical energy for fast ion redistribution by sawteeth. The redistribution of fast particles can be predicted using the criteria introduced in [29]. When the crash duration is much shorter than the precession period, trapped particles are redistributed by a sawtooth crash. Based on the condition, the critical velocity of trapped particles is defined as

$$v \ll r_{\mathrm{mix}}\omega_B \left(\frac{4\pi}{\epsilon_{\mathrm{mix}}\tau_{\mathrm{cr}}\omega_B}\right)^{1/2}, \tag{4}$$

where r_{mix} is the sawtooth mixing radius, ω_B is the ion cyclotron frequency, ϵ_{mix} is the inverse aspect ratio at the mixing radius and τ_{cr} is the duration of the sawtooth crash. For the NSTX-U discharge investigated in this work, the estimated critical energy for the redistribution of trapped particles is about 30 keV. Note that the τ_{cr} value is set to 50 μs based on the soft x-ray emission in NSTX-U (typically 40–50 μs). For passing particles, particles are not affected by sawtooth crashes if the particle velocity is greater than a critical value as shown below:

$$v \gg r_{\mathrm{mix}}\omega_B \left|q - 1\right| / G\left(\kappa\right), \tag{5}$$

where $G\left(\kappa\right)$ is the combination of the complete elliptic integrals. From this criterion, the critical energy for passing particles to have impacts from sawtooth crashes is about 1.1 MeV in this discharge.

From the ORBIT-kick modelling results, one can use the ΔP_ζ for the comparison with the theory. Using the relation between P_ζ and ψ_p ($P_\zeta = g\rho_{||} - \psi_p$), ΔP_ζ can approximate the redistribution of fast ions in real space. In order to find the critical energy for the redistribution of passing and trapped particles, the maximum value of ΔP_ζ has been evaluated for each fast ion energy. As seen in figure 12(*a*) for one energy case ($E = 47.5$ keV), four values (0.13, 0.39, 0.74, 1.0) of $\mu B_0/E$ are chosen to represent different orbit types from passing to trapped particles. The maximum ΔP_ζs for each $\mu B_0/E$ value are shown in figure 12(*b*) for fast ion energy between 10 and 400 keV. For passing particles (blue and red), the maximum values of ΔP_ζ are similar for the all energy range indicating that the critical energy for passing particles redistribution is not clearly seen in this range as predicted (critical energy $\sim$1.1 MeV). On the other hand, trapped particles show a distinct critical energy for the redistribution. The maximum values of ΔP_ζ peak around 25 keV then trapped particles with higher energies experience weaker effects from the crash (critical energy $\sim$30 keV). The violet diamond case mostly represent trapped particles and in the high energy level ($>$100 keV), the sawtooth-induced redistribution is almost negligible while the mixture of passing and trapped particles for the green triangle case allows certain level of maximum ΔP_ζ in higher energy range. Note that in NSTX-U discharges, the maximum fast ion energy is normally less than 100 keV (70 keV in #204163). In this work, for the simple comparison with theoretical predictions, the range of fast ion energy has been extended without changing other parameters such as the q profile in ORBIT and kick model.

5.3. Comparison with the recent experimental observation from MAST tokamak

As briefly mentioned in an earlier work [4], the experimental observation from MAST tokamak is not consistent with that of NSTX-U [4, 10]. Since the plasmas in both works have

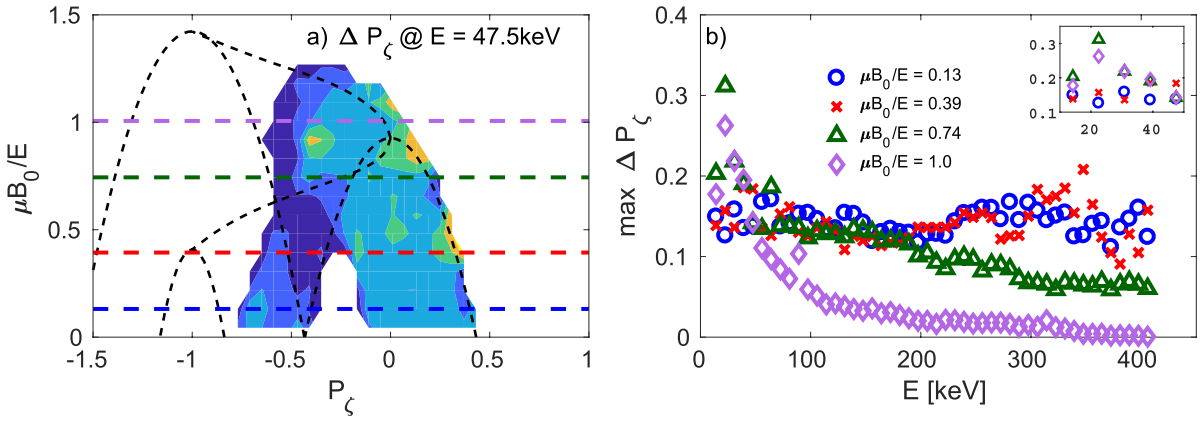

Figure 12. Four different values of $\mu B_0/E$ (0.13, 0.39, 0.74, 1.0) are taken to test the variation of the maximum values of ΔP_ζ across the change of fast ion energy. (*a*) One example of the ΔP_ζ and different $\mu B_0/E$ values at $E = 47.5$ keV. (*b*) The maximum values of ΔP_ζ from each fast ion energy show a clear critical energy for trapped particles (violet diamond, green triangle) and almost no variation for passing particles (blue circle, red cross). It is shown that the application of kick model can produce the fast ion features that predicted from a theory [29].

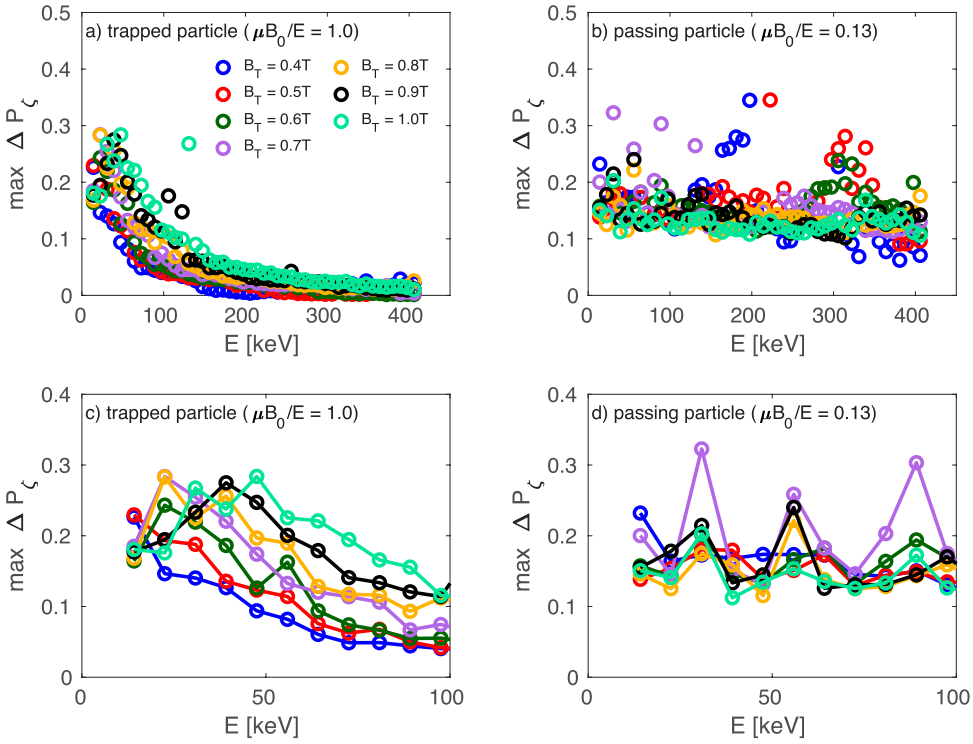

Figure 13. (*a*) The maximum values of ΔP_ζ for trapped particles decrease with increase of fast ion energy for all B_0 values. (*b*) The maximum values of ΔP_ζ stay on similar level for all energy range and B_0 values. Narrow energy window (0–100 keV) is shown (*c*) for trapped and (*d*) passing particles.

several differences such as magnetic field strength, fast ion energy, plasma profile change during sawtooth cycles, those two experimental results cannot be directly compared. In order to have an idea for the possible reason for the difference, we have carried out simple tests by changing two factors from the NSTX-U case.

Firstly, the effect of magnetic field strength B_0 has been tested. B_0 values are chosen between 0.4 and 1.0 T. It should be noted that other parameters related to the change of B_0 are not modified to keep the test simple. With various B_0 values, the scanning of fast ion energy for the maximum ΔP_ζ has been done in the same way as figure 12. The maximum ΔP_ζ for trapped and passing particles are shown in figure 13. Same as seen in figure 12, trapped particles with high energy have smaller effect from sawteeth and the maximum ΔP_ζ converges towards zero (figures 13(*a*) and (*c*) for narrow energy window) while passing particles do not show clear critical energy for the redistribution (figures 13(*b*) and (*d*) for narrow energy window). Unlike MAST experimental results, for lower B_0 cases (0.4–0.6 T), the sawtooth-induced redistribution is

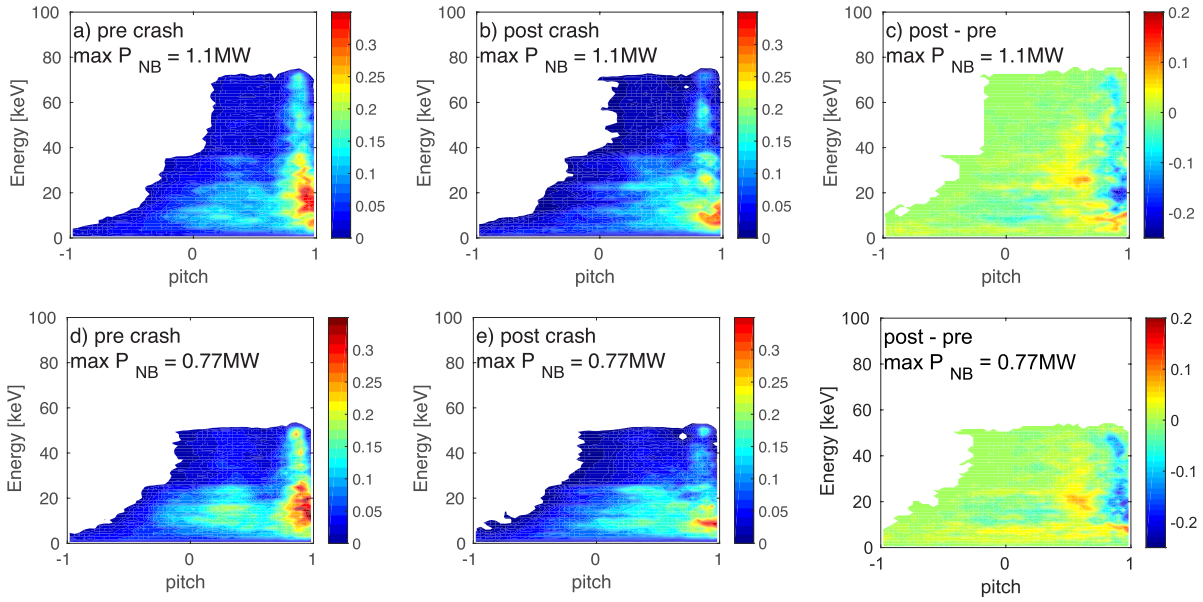

Figure 14. Fast ion distribution before and after a crash and the difference (*a*)–(*c*) for $P_{\mathrm{NB}} = 1.1$ MW and (*d*)–(*f*) for 0.77 MW. As P_{NB} decreases, the number of lower energy trapped particles increases and the difference of redistribution level for trapped and passing particles decreases.

clearly different for trapped and passing particles. From this test, B_0 seems not have significant effects on the difference between MAST and NSTX-U but for more detailed comparison, parameters related to the B_0, e.g. q profile, need to be modified as well. In addition, the possible role of wave-particle resonances with specific types of particles (e.g. passing versus trapped) on the overall fast ion transport remains an open question for future studies.

For the second test, the injected beam power P_{NB} decreases from 1.1 to 0.77 MW to reduce the NB injection energy to the MAST like value (about 50 keV). The comparison of fast ion distribution functions for the two cases are presented in figure 14, before and after a crash and the difference at the normalised radius of 0.55. In this test, the same probability matrix is applied and only P_{NB} is lowered in TRANSP. Note also that other parameters affected by the change of P_{NB} such as temperature profiles, sawtooth period are fixed. Although the critical energy for redistribution of trapped particles is still seen, the difference between the change of distribution of trapped and passing particles is smaller for lower energy case. Due to the lower neutral beam injection energy, the maximum energy of fast particles is lower. This may result in the increase of number of trapped particles that slow down to the energy lower than the critical energy. As more trapped particles are affected by a sawtooth crash, the level of redistribution can be comparable to the passing particle redistribution. For better comparison, all the possible changes need to be considered as well as equilibrium data.

Although the purpose of these tests are not to have the realistic comparison between MAST and NSTX-U, this simple comparison is worth to initiate the investigation. As diagnostics on the two devices may be looking at different regions of phase space, a meaningful comparison has to go through the full FIDASIM analysis and take into account the specific geometry of FIDA system on NSTX-U and MAST. With the exact data, it would be possible to understand why two spherical tori had very different observation.

6. Conclusions

Conventional sawtooth models implemented into time-dependent transport simulations such as TRANSP can be used to reproduce some global parameters similar to the measurements with a proper free parameter set. However, it is difficult to self-consistently predict the parameter set and detailed fast ion properties, for instance distribution function, cannot be the same if the characteristics of fast ion transport are not taken into consideration. In this work, the reduced kick model has been applied to the ORBIT code based on a NSTX-U sawtoothing discharge to find the effect of sawtooth instability and the phase space dependence on fast ion redistribution. From the ORBIT-kick modelling, the probability matrix of the change of fast ion energy and canonical momentum is calculated and is applied as an updated input parameter to NUBEAM module in TRANSP to take into account the fast ion energy and orbit type in the sawtooth-induced fast ion redistribution.

From the simulation results, it is shown that the application of the kick model can improve the modelling of fast ion transport in the sawtoothing discharges. In other words, for the proper modelling of sawtooth-induced fast ion redistribution, the phase space variables should be included in the sawtooth model. Using the kick model, the neutron rate is in a good agreement with the measurement. The fast ion related profiles and distribution function from TRANSP show clear effects from sawteeth that conventional models do not show. Comparison of FIDA simulation using the TRANSP results with FIDA measurements confirms the improvement of modelling when the kick model is applied.

The simulation results show that sawteeth mostly affect low energy trapped particles. The critical energy for the redistribution of fast ions can be estimated using the criteria in [29]. The zero-dimensional prediction can help to understand the different behaviour of fast ions, in particular trapped particles, with their energy. However, more quantitative criteria to describe the level of redistribution of fast ions after a sawtooth crash are required. ORBIT modelling is expected to find more general and quantitative criteria and it can improve kick model or help to develop a new model for fast ion transport.

Simple test simulations that investigate the different experimental observation between MAST and NSTX-U show that the difference may result from the neutral beam injection power. With lower beam power in MAST, the maximum energy of trapped particles is lower so that more particles slow down below the critical energy. As a result, the number of trapped particles that are redistributed due to a sawtooth crash can be comparable with that of passing particles. More detailed simulations as well as FIDA simulations should follow for better understanding.

Acknowledgments

This work is supported by the U.S. Department of Energy, Office of Science, Office of Fusion Energy Sciences under contract numbers DE-AC02-09CH11466, DE-FG02-06ER54867 and DE-FG03-02ER54681. NSTX-U at PPPL is a DOE Office of Science User Facility. The digital data for this paper can be found following the links from http://arks.princeton.edu/ark:/88435/dsp018p58pg29j. The publisher, by accepting the article for publication acknowledges, that the United States Government retains a non-exclusive, paid-up, irrevocable, world-wide license to publish or reproduce the published form of this manuscript, or allow others to do so, for United States Government purposes.

ORCID iDs

D. Kim https://orcid.org/0000-0002-6085-9525
M. Podestà https://orcid.org/0000-0003-4975-0585
D. Liu https://orcid.org/0000-0001-9174-7078
G. Hao https://orcid.org/0000-0003-2310-6134
F.M. Poli https://orcid.org/0000-0003-3959-4371

References

[1] Porcelli F., Boucher D. and Rosenbluth M.N. 1996 *Plasma Phys. Control. Fusion* **38** 2163
[2] Menard J. *et al* 2012 *Nucl. Fusion* **52** 083015
[3] Battaglia D. *et al* 2018 *Nucl. Fusion* **58** 046010
[4] Liu D. *et al* 2018 *Nucl. Fusion* **58** 082028
[5] Muscatello C. *et al* 2012 *Plasma Phys. Control. Fusion* **54** 025006
[6] Geiger B. *et al* 2014 *Nucl. Fusion* **54** 022005
[7] Jaulmes F. *et al* 2016 *Nucl. Fusion* **56** 112012
[8] Rasmussen J. *et al* 2016 *Nucl. Fusion* **56** 112014
[9] Nielsen S. *et al* 2010 *Plasma Phys. Control. Fusion* **52** 092001
[10] Cecconello M., Sperduti A. and the MAST Team 2018 *Plasma Phys. Control. Fusion* **60** 055008
[11] Hawryluk R. 1980 *An Empirical Approach to Tokamak Transport Physics Close to Thermonuclear Conditions* vol 1, ed B. Coppi *et al* (Brussels: Commission of the European Communities) p 19
[12] Breslau J., Gorelenkova M., Poli F., Sachdev J. and Yuan X. 2018 TRANSP [Computer Software] (https://doi.org/10.11578/dc.20180627.4)
[13] Kadomtsev B. 1975 *Sov. J. Plasma Phys.* **1** 710
[14] Bortolon A., Heidbrink W. and Podestà M. 2010 *Rev. Sci. Instrum.* **81** 10D728
[15] Podestà M., Heidbrink W., Bell R. and Feder R. 2008 *Rev. Sci. Instrum.* **79** 10E521
[16] Heidbrink W.W., Liu D., Luo Y., Ruskov E. and Geiger B. 2011 *Commun. Comput. Phys.* **10** 716
[17] White R. and Chance M.S. 1984 *Phys. Fluids* **27** 2455
[18] Kim D., Podestà M., Liu D. and Poli F. 2018 *Nucl. Fusion* **58** 082029
[19] Podestà M., Gorelenkova M. and White R. 2014 *Plasma Phys. Control. Fusion* **56** 055003
[20] Podestà M., Gorelenkova M., Gorelenkov N. and White R. 2017 *Plasma Phys. Control. Fusion* **59** 095008
[21] Goldston R. *et al* 1981 *J. Comput. Phys.* **43** 61
[22] Pankin A. *et al* 2004 *Comput. Phys. Commun.* **159** 157
[23] LeBlanc B. 2008 *Rev. Sci. Instrum.* **79** 10E737
[24] Bell R. *et al* 2010 *Phys. Plasmas* **17** 082507
[25] Liu D. *et al* 2014 *Rev. Sci. Instrum.* **85** 11E105
[26] Liu D. *et al* 2016 *Rev. Sci. Instrum.* **87** 11D803
[27] White R. 2013 *Phys. Plasmas* **20** 022105
[28] White R. 2014 *The Theory of Toroidally Confined Plasmas* 3rd edn (London: Imperial College Press)
[29] Kolesnichenko Y.I., Lutsenko V. and Yakovenko Y.V. 1997 *Phys. Plasmas* **4** 2544
[30] LoDestro L. and Pearlstein L. 1994 *Phys. Plasmas* **1** 90
[31] Heidbrink W., Ruskov E., Liu D., Stagner L., Fredrickson E., Podestà M. and Bortolon A. 2016 *Nucl. Fusion* **56** 056005